Research Square

Preprints are preliminary reports that have not undergone peer review.
They should not be considered conclusive, used to inform clinical practice,
or referenced by the media as validated information.

Diagnostic Value of Combined Automated Breast Ultrasound System and Conventional Two-Dimensional Ultrasound for Intraductal Breast Lesions

Qiuya Yang
Department of Ultrasound,The First Medical Center of Chinese PLA General Hospital
Ran Yi
Department of Ultrasound,The First Medical Center of Chinese PLA General Hospital
Feiyue Guo
Department of Ultrasound,The First Medical Center of Chinese PLA General Hospital
Taohua Gou
Department of Ultrasound,The First Medical Center of Chinese PLA General Hospital
Lei Cai
Department of Ultrasound,The First Medical Center of Chinese PLA General Hospital
Shuo Wang
Department of Ultrasound,The First Medical Center of Chinese PLA General Hospital
Yan Zhang
Department of Ultrasound,The First Medical Center of Chinese PLA General Hospital
Yukun Luo
lyk301@163.com

Department of Ultrasound,The First Medical Center of Chinese PLA General Hospital

Research Article

Keywords: Automated Breast Ultrasound System, two-dimensional ultrasound, intraductal breast lesion

Posted Date: June 28th, 2026

DOI: https://doi.org/10.21203/rs.3.rs-9936589/v1

License: This work is licensed under a Creative Commons Attribution 4.0 International License.
Read Full License

Additional Declarations: No competing interests reported.

Version of Record: A version of this preprint was published at BMC Medical Imaging on October 20th, 2026. See the published version at https://doi.org/10.1186/s12880-026-02832-z.

Abstract

Objective

To explore the clinical value of Automated Breast Ultrasound System (ABUS) combined with two-dimensional ultrasound for intraductal breast lesions, and to provide imaging evidence for preoperative benign and malignant differentiation.

Methods

Patients with pathologically confirmed intraductal breast lesions hospitalized in our hospital from April 2025 to April 2026 were enrolled. All subjects underwent two-dimensional ultrasound and ABUS examination. Ultrasonographic features were compared between benign and malignant groups. Univariate and multivariate logistic regression were used to screen independent risk factors of malignant lesions and establish a combined diagnostic model. ROC curves were drawn to compare the diagnostic efficiency of different detection schemes.

Results

A total of 200 patients were enrolled, including 132 benign cases and 68 malignant cases. The malignant group had significantly higher incidences of irregular shape, microcalcification, abundant blood flow, duct dilatation ≥ 5 mm, convergence sign, nipple-oriented lesion extension and marginal spiculation or angulation ($P < 0.05$). Multivariate logistic regression confirmed seven independent risk factors for malignancy ($P < 0.05$): irregular lesion morphology, microcalcification, Adler grade II–III blood flow, duct dilatation ≥ 5 mm, convergence sign, lesion extending toward the nipple and spiculation/angulation. The combined model had an AUC of 0.90, superior to standalone two-dimensional ultrasound (AUC = 0.81) and single ABUS (AUC = 0.86), with sensitivity of 90.7% and specificity of 89.2%.

Conclusion

Combination of ABUS and two-dimensional ultrasound has prominent clinical value for differentiating benign and malignant intraductal breast lesions, which improves preoperative diagnostic accuracy and facilitates clinical decision-making.

Introduction

Intraductal breast lesions originate from mammary duct epithelium, consisting of benign lesions (usual ductal hyperplasia, intraductal papilloma), premalignant lesions (atypical ductal hyperplasia) and malignant lesions (ductal carcinoma in situ, DCIS with microinvasion)[1–3]. Most early lesions present non-specific manifestations including nipple discharge, palpable nodules or no obvious symptoms.

Accurate preoperative differentiation of benign and malignant lesions contributes to individualized treatment and better clinical prognosis[4–6].

As a routine screening tool for breast disorders, conventional two-dimensional ultrasound is non-invasive, convenient and repeatable. It clearly displays lesion morphology, margin, internal echo and blood flow, serving as the primary imaging modality for intraductal lesion evaluation[7–9]. Nevertheless, it only provides planar images and cannot completely display three-dimensional duct structure and overall lesion infiltration, leading to diagnostic limitations for tiny and atypical lesions[10–12].

Three-dimensional automated breast volume scanning overcomes the defects of two-dimensional ultrasound. With three-dimensional reconstruction and exclusive coronal imaging, ABUS clearly demonstrates lesion margin, microcalcification and duct dilatation; coronal view accurately delineates the distribution of microcalcification and helps determine lesion nature and invasion scope[13–15]. However, existing researches mostly focus on the diagnostic performance of single ultrasound modality, while few studies combine two-dimensional and ABUS indicators to build systematic diagnostic models for intraductal lesions[6, 9].

Using pathological outcomes as the reference gold standard, our study integrates two-dimensional and ABUS ultrasonic features to screen independent malignant risk factors and establish a combined diagnostic model. Diagnostic efficiencies of single and combined examinations are compared to provide a practical preoperative imaging scheme for intraductal breast lesions.

Materials and Methods

1 Study Population

This study was approved by the Institutional Ethics Committee of the First Medical Center, Chinese PLA General Hospital (No. S2025-1127-01) and performed in accordance with the Declaration of Helsinki. All enrolled patients signed written informed consent before examinations. A total of 200 patients with pathologically-confirmed intraductal breast lesions from April 2025 to April 2026 were enrolled after receiving both two-dimensional ultrasound and ABUS scanning.Fig. 1

Inclusion criteria: (1) Complete two-dimensional and ABUS examinations with high-quality images available for feature analysis; (2) Definite pathological diagnosis of benign or malignant lesions; (3) No prior breast surgery, radiotherapy or chemotherapy; (4) No history of other malignant tumors; (5) Complete clinical and follow-up data.

Exclusion criteria: (1) Poor-quality ultrasound images unable for feature identification; (2) Uncertain pathological diagnosis; (3) Severe comorbidities of heart, liver or renal dysfunction; (4) Pregnant or lactating women.

2 Examination Protocols and Observation Indexes

Two-dimensional ultrasound was performed on Mindray Resona 7 with L14-5 linear probe (7–14 MHz, frame rate=20 fps). ABUS scanning was carried out on IBUS BE3 automated breast volume system with 13L5BV probe (5–12 MHz, scanning area:13 cm×17 cm, slice thickness:0.1 mm). All images were independently reviewed by two experienced sonographers (≥5 years' breast ultrasound experience) under blind condition without pathological information; disputed findings were adjudicated by a third senior radiologist.

2.1 Conventional Two-dimensional Ultrasound

Patients were placed in supine position with arms elevated for full breast scanning across all quadrants. Observed indicators contained lesion size, location, margin, morphology, internal echo homogeneity, calcification, duct dilatation status and dilated width, blood flow in solid lesion and intraductal vascularity. Blood flow was graded by Adler classification: Grade 0 (no blood flow); Grade I (1–2 punctate or linear small vessels); Grade II (3–4 punctate vessels or one main vascular trunk); Grade III (≥5 punctate vessels or ≥2 major feeding vessels).

2.2 ABUS Three-dimensional Ultrasound

Semi-supine position was adopted for full-breast volumetric scanning; coronal, sagittal and transverse images were reconstructed for analysis. Recorded ABUS features included lesion morphology, duct dilatation, convergence sign, nipple-oriented lesion extension, spiculation/angulation and peripheral hyperechoic rim.

2.3 Uniform Image Interpretation Criteria

Convergence sign: Perilesional breast parenchyma radially converges toward the central lesion on ABUS coronal plane, indicating invasive growth along duct system.

Spiculation/angulation: Irregular cord-like protrusions or sharp angular changes at lesion margin, representing interstitial infiltration of malignant cells.

Nipple-oriented extension: Lesion long axis stretches along mammary duct toward or connects directly with nipple.

Microcalcification: Punctate high-echo foci <1 mm inside lesions or duct walls, isolated or clustered.

Marked duct dilatation: Duct inner diameter ≥2 mm; dilatation width ≥5 mm is defined as severe duct ectasia[1].

3 Statistical Analysis

All statistical analyses were completed with SPSS 26.0. Measurement data were expressed as mean±standard deviation and compared by independent-sample t-test; enumeration data were presented as case number (percentage) and analyzed via χ^2 test. Kappa coefficient was used to evaluate

inter-observer consistency of categorical indicators, while ICC for quantitative measurements. Variables with P<0.05 in univariate analysis were included in multivariate logistic regression after multicollinearity test to screen independent malignant risk factors. ROC curves were plotted, DeLong test was used for pairwise AUC comparison, and sensitivity, specificity, positive predictive value (PPV) and negative predictive value (NPV) were calculated. P<0.05 was considered statistically significant.

Results

All 200 enrolled patients were female and divided into benign group (n=132) and malignant group (n=68) according to pathological findings. Benign group contained 58 usual ductal hyperplasia, 62 intraductal papilloma and 12 atypical ductal hyperplasia (age:32–58 y, mean 45.2±6.8 y). Malignant group included 49 pure DCIS and 19 DCIS with microinvasion (age:38–62 y, mean 48.7±7.3 y). No significant intergroup difference was found in age and lesion location (P>0.05). For lesion size: 85 lesions <1 cm and 47 ≥1 cm in benign group; 18 <1 cm and 50 ≥1 cm in malignant group (P>0.05). Duct dilatation was detected in 30 benign and 50 malignant lesions on two-dimensional ultrasound (P<0.05), and in 28 benign and 39 malignant lesions on ABUS (P<0.05). Lesion location had no correlation with malignant risk (P>0.05).

1 Inter-observer Consistency of Image Interpretation

Kappa=0.81 for qualitative feature evaluation and ICC=0.87 for quantitative measurement between two radiologists, showing excellent inter-rater agreement (P<0.05).

2 Comparison of Ultrasonic Features Between Two Groups

Significant intergroup differences were observed in margin, morphology, echo, homogeneity, calcification, blood flow and duct dilatation on two-dimensional ultrasound (P<0.05), while lesion size, location and uniformity of duct dilatation showed no statistical difference (P>0.05).Table 1 On ABUS, significant differences existed in margin, morphology, echo, calcification, duct dilatation, convergence sign, nipple-oriented extension, spiculation/angulation and peripheral hyperechoic rim (P<0.05). Table 2

Univariate screening identified seven statistically different indicators between two cohorts; multivariate logistic regression confirmed irregular morphology, microcalcification, grade II–III blood flow, duct dilatation ≥5 mm, convergence sign, nipple-directed extension and spiculation/angulation as independent malignant risk factors (P<0.05).Fig. 2

3 Diagnostic Efficacy of Different Examination Schemes

With pathological diagnosis as gold standard, ROC analysis revealed combined model AUC=0.90 (95%CI:0.85–0.94), superior to two-dimensional ultrasound (AUC=0.81,95%CI:0.74–0.87) and standalone ABUS (AUC=0.86,95%CI:0.80–0.91, P<0.05). The combined model achieved sensitivity of 90.7% and specificity of 89.2%, exceeding single two-dimensional ultrasound (81.5% sensitivity,84.2% specificity) and single ABUS (87.0% sensitivity,88.3% specificity). Table 3, Fig. 3

Discussion

Typical imaging manifestations of benign and malignant intraductal breast lesions are illustrated in the representative cases below (Fig. 4).

Conventional two-dimensional ultrasound only provides sectional images and fails to fully display three-dimensional duct anatomy and multifocal lesion extension, restricting its diagnostic performance for non-mass and tiny intraductal lesions[16–18]. ABUS overcomes such drawbacks via automatic full-breast scanning and coronal reconstruction, realizing panoramic visualization of duct tree and benefiting dense-breast population screening[19, 20]. Previous studies verified that coronal-specific signs including convergence sign and spiculation improve detection sensitivity of DCIS by 12%–18% compared with two-dimensional ultrasound[21,22]. The seven independent malignant predictors identified in our research are closely correlated with tumor proliferation and interstitial invasion[2,23–24].

Irregular morphology serves as the strongest malignant predictor, pathologically caused by invasive tumor growth along duct epithelium and destroyed normal duct structure[25]. High-incidence irregular contour (89.2%) in malignant lesions is distinctly higher than benign counterparts (23.5%)[26]. Microcalcification rate reached 54.4% in malignant group versus 6.8% in benign group, consistent with published data ranging from 50% to 60%, originating from tumor ischemic necrosis and intraductal secretion mineralization[27]. Grade II–III hypervascularity results from VEGF-mediated abnormal angiogenesis and correlates with high Ki-67 index, consistent with Mo's research[28]. Duct dilatation ≥ 5 mm arises from persistent tumor compression and duct wall destruction; the 5 mm cutoff value has been validated in former literature[1].

Coronal-specific ABUS signs possess unique pathological implication for malignant diagnosis[16]. Convergence sign reflects parenchymal traction induced by tumor infiltration along duct system with specificity up to 83.9%[22]. Nipple-oriented lesion extension corresponds to segmental multicentric growth of DCIS, and spiculation/angulation directly manifests interstitial cancer invasion. These features are easily missed or misdiagnosed on two-dimensional limited sectional scanning, whereas panoramic ABUS coronal view markedly improves diagnostic accuracy for atypical lesions[20].

Combined two-dimensional ultrasound and ABUS obtained an AUC of 0.90 with sensitivity 90.7% and specificity 89.2%, significantly superior to single-modality ultrasound. Two-dimensional ultrasound depicts internal echo and blood flow details, while ABUS provides three-dimensional duct morphology and characteristic malignant coronal signs; complementary combination reduces misdiagnosis of iso-echoic, tiny and diffuse intraductal lesions.

Lesion location showed no correlation with malignancy, which reminds clinicians not to judge lesion nature by anatomical site. Although duct dilatation is not an exclusive malignant feature, dilatation ≥ 5 mm indicates significantly elevated malignant risk.

Limitations: This is a single-center retrospective study with limited sample size (n = 200), leading to potential selection bias; no head-to-head comparison with mammography or breast MRI; subjective bias exists in artificial image interpretation despite blind evaluation. Future multi-center prospective researches with external validation cohorts are required to verify the diagnostic model; radiomics and artificial intelligence can be applied to develop automatic intelligent diagnostic system.

Conclusion

Combination of ABUS and two-dimensional ultrasound compensates respective defects and improves preoperative discrimination of intraductal breast lesions. The seven screened ultrasonic risk factors help sonographers establish standardized imaging-pathology cognition and optimize clinical treatment strategy.

Declarations

Human Ethics and Consent to Participate declarations

Ethical approval for this study was obtained from the Institutional Ethics Committee of the First Medical Center, Chinese PLA General Hospital (Approval No. S2025-1127-01). The study was conducted following the principles of the Declaration of Helsinki. Written informed consent was obtained from all individual participants included in the study.

Funding declaration

No funding was received for this study.

Author Contribution

Qiuya Yang and Ran Yi: Study design, data collection, image analysis, manuscript drafting (Co-first authors).Feiyue Guo, TaoHua Gou, Lei Cai, Shuo Wang: Patient screening, ultrasound image review, statistical data sorting.Yan Zhang and Yukun Luo: Project supervision, research design revision, critical revision of manuscript, funding support and final approval of the article (Co-corresponding authors).All authors have read and approved the final submitted manuscript. No conflicts of interest exist among all contributors.

Data Availability

Availability of Data and MaterialsThe original patient ultrasound imaging and clinical data cannot be shared publicly because of ethical constraints and patient confidentiality policies. Access to de-identified

research data is available from the corresponding author upon reasonable request and institutional ethics approval. All data generated or analysed during this study are included in this published article.

References

1. Choudhery S, Simmons C, Woodard GA, Bhatt AA, Anderson TL, Lee CU. Outcomes of solitary dilated breast ducts in symptomatic and asymptomatic patients. Br J Radiol. 2020 May 1;93(1109):20191039. doi: 10.1259/bjr.20191039. Epub 2020 Feb 28. PMID: 32101458; PMCID: PMC7217566.
2. Oba K, Tsunoda H, Moon WK. Ductal abnormalities as primary findings on breast ultrasonography: a literature review and proposed classification. Ultrasonography. 2025 Jul;44(4):245-259. doi: 10.14366/usg.25048. Epub 2025 May 6. PMID: 40534164; PMCID: PMC12242359.
3. Hamwi MW, Winters R. Mammary Duct Ectasia. 2023 Jul 17. In: StatPearls [Internet]. Treasure Island (FL): StatPearls Publishing; 2026 Jan–. PMID: 32491597.
4. Moseley TW, Adrada BE, Arribas EM, Chung HL, Kapoor MM, Patel MM, Ghannam S, Guirguis MS. Solitary Dilated Ducts 2.0 - Multimodality Imaging Detection, Assessment, and Management. J Breast Imaging. 2025 Oct 28;7(5):606-618. doi: 10.1093/jbi/wbaf012. PMID: 40884407.
5. Hsu HH, Yu JC, Hsu GC, Chang WC, Yu CP, Tung HJ, Tzao C, Huang GS. Ultrasonographic alterations associated with the dilatation of mammary ducts: feature analysis and BI-RADS assessment. Eur Radiol. 2010 Feb;20(2):293-302. doi: 10.1007/s00330-009-1546-8. Epub 2009 Aug 26. PMID: 19707771.
6. You C, Shen Y, Sun S, Zhou J, Li J, Su G, Michalopoulou E, Peng W, Gu Y, Guo W, Cao H. Artificial intelligence in breast imaging: Current situation and clinical challenges. Exploration (Beijing). 2023 Jul 20;3(5):20230007. doi: 10.1002/EXP.20230007 PMID: 37933287; PMCID: PMC10582610.
7. Chamming's F, Mesurolle B, Antonescu R, Aldis A, Kao E, Thériault M, Omeroglu A, Pinel-Giroux F, Seidler M, Solorzano S, Reinhold C, Gallix B. Value of Shear Wave Elastography for the Differentiation of Benign and Malignant Microcalcifications of the Breast. AJR Am J Roentgenol. 2019 Aug;213(2):W85-W92. doi: 10.2214/AJR.18.20899. Epub 2019 Apr 30. PMID: 31039014.
8. Ban K, Tsunoda H, Watanabe T, Kaoku S, Yamaguchi T, Ueno E, Hirokaga K, Tanaka K. Characteristics of ultrasonographic images of ductal carcinoma in situ with abnormalities of the ducts. J Med Ultrason (2001). 2020 Jan;47(1):107-115. doi: 10.1007/s10396-019-00981-z. Epub 2019 Oct 26. PMID: 31655940; PMCID: PMC6971153.
9. Watanabe T, Yamaguchi T, Tsunoda H, Kaoku S, Tohno E, Yasuda H, Ban K, Hirokaga K, Tanaka K, Umemoto T, Okuno T, Fujimoto Y, Nakatani S, Ito J, Ueno E. Ultrasound Image Classification of Ductal Carcinoma In Situ (DCIS) of the Breast: Analysis of 705 DCIS Lesions. Ultrasound Med Biol. 2017 May;43(5):918-925. doi: 10.1016/j.ultrasmedbio.2017.01.008. Epub 2017 Feb 24. PMID: 28242086.
10. Li W, Zhou Q, Xia S, Wu Y, Fei X, Wang Y, Tao L, Fan J, Zhou W. Application of Contrast-Enhanced Ultrasound in the Diagnosis of Ductal Carcinoma In Situ: Analysis of 127 Cases. J Ultrasound Med.

2020 Jan;39(1):39-50. doi: 10.1002/jum.15069. Epub 2019 Jun 17. PMID: 31206200.

11. Li Q, Hu M, Chen Z, Li C, Zhang X, Song Y, Xiang F. Meta-Analysis: Contrast-Enhanced Ultrasound Versus Conventional Ultrasound for Differentiation of Benign and Malignant Breast Lesions. Ultrasound Med Biol. 2018 May;44(5):919-929. doi: 10.1016/j.ultrasmedbio.2018.01.022. Epub 2018 Mar 9. PMID: 29530434.
12. Wang B, Yang D, Zhang X, Gong X, Xu T, Han J, Ren Y, Zou S, Li L, Wang Y. The diagnostic value of contrast-enhanced ultrasonography in breast ductal abnormalities. Cancer Imaging. 2023 Mar 10;23(1):25. doi: 10.1186/s40644-023-00539-w. PMID: 36899406; PMCID: PMC10007791.
13. Guo S, Zhou X, Zhou J, Gong L, Zhou S, Jiang L, Zhang Y, Jin L, Zhou P. Multimodal combined model integrating 2.5D deep learning and habitat radiomics for malignancy discrimination in ≤2 cm BI-RADS 4 breast lesions. Quant Imaging Med Surg. 2026 May 1;16(5):377. doi: 10.21037/qims-2025-1-2812. Epub 2026 Apr 14. PMID: 42147917; PMCID: PMC13178382.
14. Tian C, Wu J, Wang Z. Diagnostic value of automated breast volume scanner for breast ductal carcinoma in situ. Medicine (Baltimore). 2025 Nov 7;104(45):e45499. doi: 10.1097/MD.0000000000045499. PMID: 41204507; PMCID: PMC12599787.
15. Wei W, Xia F, Zhou W, Lu W, Zhang D, Ma Q, Xu X, Zhang C. *Ki-67* Prediction in Breast Cancer: Integrating Radiomics From Automated Breast Volume Scanner and 2D Ultrasound Images via Machine Learning. Breast Cancer (Dove Med Press). 2025 Oct 11;17:897-912. doi: 10.2147/BCTT.S540595. PMID: 41104393; PMCID: PMC12523655.
16. Zhang H, Hu J, Meng R, Liu F, Xu F, Huang M. A systematic review and meta-analysis comparing the diagnostic capability of automated breast ultrasound and contrast-enhanced ultrasound in breast cancer. Front Oncol. 2024 Jan 9;13:1305545. doi: 10.3389/fonc.2023.1305545 PMID: 38264749; PMCID: PMC10803446.
17. Rajkumar R, Singh T, Singla V, Singh G, Bal A, Khandelwal N. Diagnostic Utility of Automated Breast Volume Scan in Differentiating Benign and Malignant Breast Masses. Cureus. 2025 Jul 2;17(7):e87191. doi: 10.7759/cureus.87191 PMID: 40755588; PMCID: PMC12316573.
18. Wang XL, Tao L, Zhou XL, Wei H, Sun JW. Initial experience of automated breast volume scanning (ABVS) and ultrasound elastography in predicting breast cancer subtypes and staging. Breast. 2016 Dec;30:130-135. doi: 10.1016/j.breast.2016.09.012. Epub 2016 Oct 6. PMID: 27718417.
19. Su L, Xie Q, Yi A, Zhang Q, Chen J. Ultrasound characteristics comparison and development of a predictive nomogram for intraductal papilloma and ductal carcinoma *in situ*: a retrospective cohort study. Front Oncol. 2025 Apr 17;15:1454951. doi: 10.3389/fonc.2025.1454951 PMID: 40313250; PMCID: PMC12043480.
20. Shiyan G, Liqing J, Yueqiong Y, Yan Z. A clinical-radiomics nomogram based on multimodal ultrasound for predicting the malignancy risk in solid hypoechoic breast lesions. Front Oncol. 2023 Oct 17;13:1256146. doi: 10.3389/fonc.2023.1256146. PMID: 37916158; PMCID: PMC10616876.
21. Kwon BR, Chang JM, Kim SY, Lee SH, Shin SU, Yi A, Cho N, Moon WK. Utility and Diagnostic Performance of Automated Breast Ultrasound System in Evaluating Pure Non-Mass Enhancement

on Breast Magnetic Resonance Imaging. Korean J Radiol. 2020 Nov;21(11):1210-1219. doi: 10.3348/kjr.2019.0881 Epub 2020 Jul 22. PMID: 32729267; PMCID: PMC7462763.

22. Suzuki M, Nakayama R, Namba K, Kawami H, Nara M, Nakamura S. Potential Usefulness a Coronal View using an Automated Breast Ultrasound System in Detecting Breast Lesions. Eur J Breast Health. 2023 Dec 27;20(1):57-63. doi: 10.4274/ejbh.galenos.2023.2023-11-6. PMID: 38187110; PMCID: PMC10765468.
23. Wang LC, Sullivan M, Du H, Feldman MI, Mendelson EB. US appearance of ductal carcinoma in situ. Radiographics. 2013 Jan-Feb;33(1):213-28. doi: 10.1148/rg.331125092. PMID: 23322838.
24. Li JK, Wang HF, He Y, Huang Y, Liu G, Wang ZL. Ultrasonographic features of ductal carcinoma in situ: analysis of 219 lesions. Gland Surg. 2020 Dec;9(6):1945-1954. doi: 10.21037/gs-20-428 PMID: 33447545; PMCID: PMC7804561
25. Cha H, Chang YW, Lee EJ, Hwang JY, Kim HJ, Lee EH, Ryu JK. Ultrasonographic features of pure ductal carcinoma in situ of the breast: correlations with pathologic features and biological markers. Ultrasonography. 2018 Oct;37(4):307-314. doi: 10.14366/usg.17039. Epub 2017 Oct 13. PMID: 29169230; PMCID: PMC6177689.
26. Liu T, Shen H, Li J, Li R, Hong X, Hu Y, Zhang S, Chen T, Liang W. Predictive value of ABVS and VTIQ parameters for axillary lymph node metastasis in breast cancer. Front Cell Dev Biol. 2026 Apr 10;14:1635743. doi: 10.3389/fcell.2026.1635743. PMID: 42039148; PMCID: PMC13106202.
27. Pu Q, Li P, Su M, Gao D. Analysis of the clinicopathological and imaging features in breast intraductal papillary lesions with or without pathological nipple discharge. Sci Rep. 2025 Jan 20;15(1):2478. doi: 10.1038/s41598-025-87278-z. PMID: 39833359; PMCID: PMC11747485.
28. Mo S, Wang M, Li G, Tian H, Wu H, Tang S, Zou X, Shao M, Xu J, Huang Z, Dong F. Noninvasive prediction of Ki67 proliferation index in breast cancer based on integrated photoacoustic imaging. BMC Med Imaging. 2026 May 22. doi: 10.1186/s12880-026-02462-5. Epub ahead of print. PMID: 42174497.

Tables

Table 1 Comparison of two-dimensional ultrasonic features between benign and malignant intraductal breast lesions

Lesion characteristics	Benign (n=132)	Malignant (n=68)	Statistic	P-value
Age	45.2±6.8	48.7±7.3	t□1.96	0.051
Size			χ²□28.36	□0.001
x□1cm	85□64.4%□	18□26.5%□		
x≥1cm	47□35.6%□	50□73.5%□		
Location			χ²□18.36	□0.001
Central nipple	27□20.5%□	22 (32.4%)		
Peripheral nipple	35□26.5%□	25 (36.8%)		
Others	70□53.0%□	21 (30.9%)		
Boundary			χ²□50.23	□0.001
Clear	98 (74.2%)	15 (22.1%)		
Unclear	34 (25.8%)	53 (77.9%)		
Shape			χ²□42.15	□0.001
Regular	89 (67.4%)	12 (17.6%)		
Irregular	43 (32.6%)	56 (82.4%)		
Echo			χ²□49.37	□0.001
Hypoechoic	43 (32.6%)	54 (79.4%)		
Isoechoic	62 (47.0%)	9 (13.2%)		
Hyperechoic	27 (20.5%)	5 (7.4%)		
Homogeneity			χ²□48.52	□0.001
Yes	85 (64.4%)	14 (20.6%)		
No	47 (35.6%)	54 (79.4%)		
Calcification			χ²□56.72	□0.001
Yes	9 (6.8%)	37 (54.4%)		
No	123 (93.2%)	31 (45.6%)		
CDFI in solid echo areas			χ²□59.83	□0.001
Grade 0-I	107 (81.1%)	19 (27.9%)		
Grade II-III	25 (18.9%)	49 (72.1%)		

CDFI within the lumen			χ^2=48.95	<0.001
Grade 0-I	25 (83.3%)	15 (30.0%)		
Grade II-III	5 (16.7%)	35 (70.0%)		
ductal dilatation			χ^2=45.62	<0.001
Yes	30 (22.7%)	50 (73.5%)		
No	102 (77.3%)	18 (26.5%)		
Uniform ductal dilatation			χ^2=18.79	0.258
Yes	22 (73.3%)	12(24.0%)		
No	8 (26.7%)	38 (76.0%)		
Width of ductal dilatation			χ^2=12.35	<0.001
≥5mm	6(20.0%)	31(62.0%)		
<5mm	24(80.0%)	19(38.0%)		

Table 2 Comparison of ABUS three-dimensional ultrasonic features between benign and malignant intraductal breast lesions

Lesion characteristics	Benign Group (n=132)	Malignant Group (n=68)	Statistic	P-value
Lesion Size			χ²□28.36	□0.001
□1cm	85□64.4%□	18□26.5%□		
≥1cm	47□35.6%□	50□73.5%□		
Location			χ²□18.36	□0.001
Central Nipple Area	27□20.5%□	22 (32.4%)		
Peripheral Nipple Area	35□26.5%□	25 (36.8%)		
Others	70□53.0%□	21 (30.9%)		
Boundary			χ²□50.23	□0.001
Clear	98 (74.2%)	15 (22.1%)		
Unclear	34 (25.8%)	53 (77.9%)		
Shape			χ²□42.15	□0.001
Regular	89 (67.4%)	12 (17.6%)		
Irregular	43 (32.6%)	56 (82.4%)		
Echo			χ²□49.37	□0.001
Hypoechoic	43 (32.6%)	54 (79.4%)		
Isoechoic	62 (47.0%)	9 (13.2%)		
Hyperechoic	27 (20.5%)	5 (7.4%)		
Homogeneity			χ²□48.52	□0.001
Homogeneous	85 (64.4%)	14 (20.6%)		
Inhomogeneous	47 (35.6%)	54 (79.4%)		
Calcification			χ²□56.72	□0.001
Present	9 (6.8%)	37 (54.4%)		
Absent	123 (93.2%)	31 (45.6%)		
With Ductal Dilatation			χ²=26.74	<0.001
Yes	28	39		
No	104	29		
Uniformity of Ductal Dilatation			χ²=1.28	0.258

Uniform	22	8		
Non-uniform	6	31		
Width of Ductal Dilatation			χ^2=53.69	<0.001
≥5mm	6	31		
5mm	22	8		
Convergence Sign			χ^2=68.42	<0.001
Present	11(8.3%)	38(55.9%)		
Absent	121(91.7%)	30(44.1%)		
Lesion Long Axis Pointing/Involving Nipple			χ^2=59.71	<0.001
Yes	15(11.4%)	35(51.5%)		
No	117(88.6%)	33(48.5%)		
Spiculation/Angulation			χ^2=72.36	<0.001
Present	9(6.8%)	41(60.3%)		
Absent	123(93.2%)	27(39.7%)		
Peripheral Echo Enhancement			χ^2=47.85	<0.001
Present	13(9.8%)	35(51.5%)		
Absent	119(90.2%)	33(48.5%)		

Table 3 Diagnostic efficacy of two-dimensional ultrasound, standalone ABUS and combined model for intraductal breast lesions

Diagnostic Methods	AUC (95%CI)	Sensitivity (%)	Specificity (%)	Positive Predictive Value (%)	Negative Predictive Value (%)	P-value
Two-Dimensional Ultrasound (2D)	0.81 (0.74-0.87)	81.5	84.2	83.0	82.8	<0.001
Three-Dimensional Ultrasound (3D)	0.86 (0.80-0.91)	87.0	88.3	88.1	87.2	0.021
Combined Diagnostic Model (2D+3D)	0.90 (0.85-0.94)	90.7	89.2	90.0	89.9	<0.001

Figures

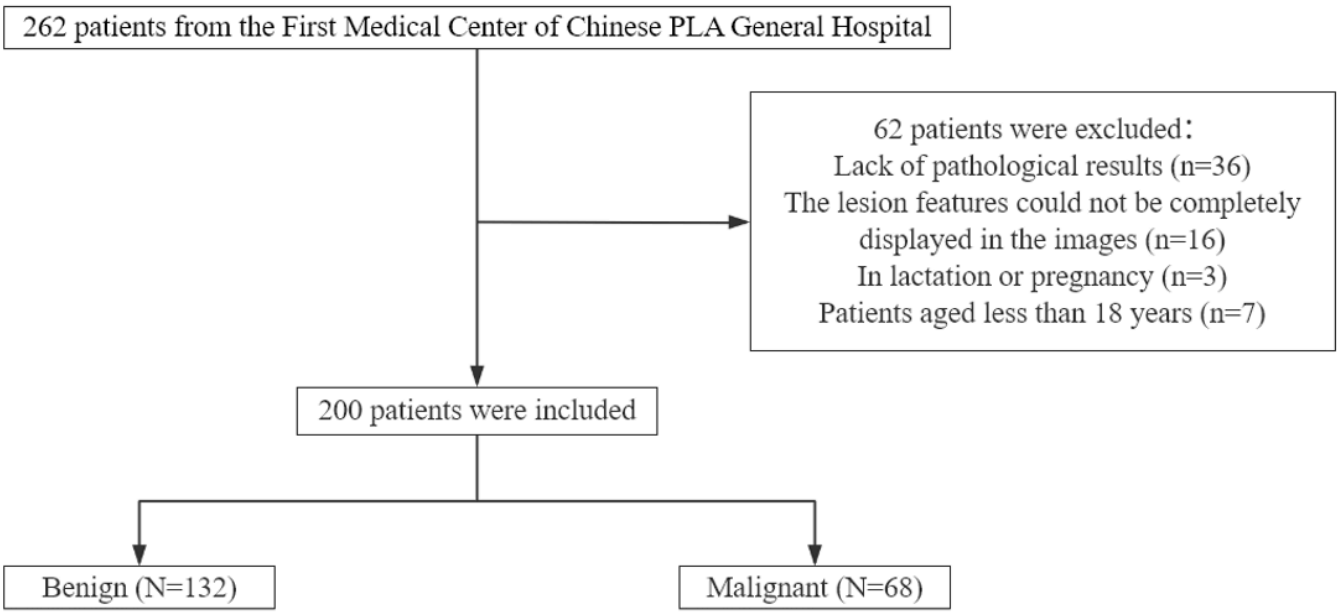


Figure 1

CONSORT flow diagram of patient enrollment and screening

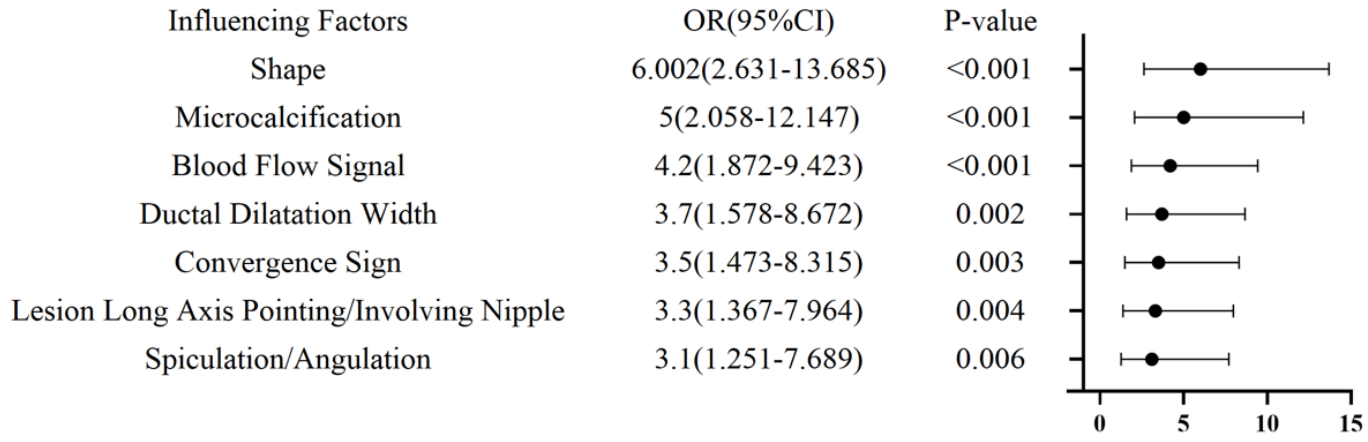
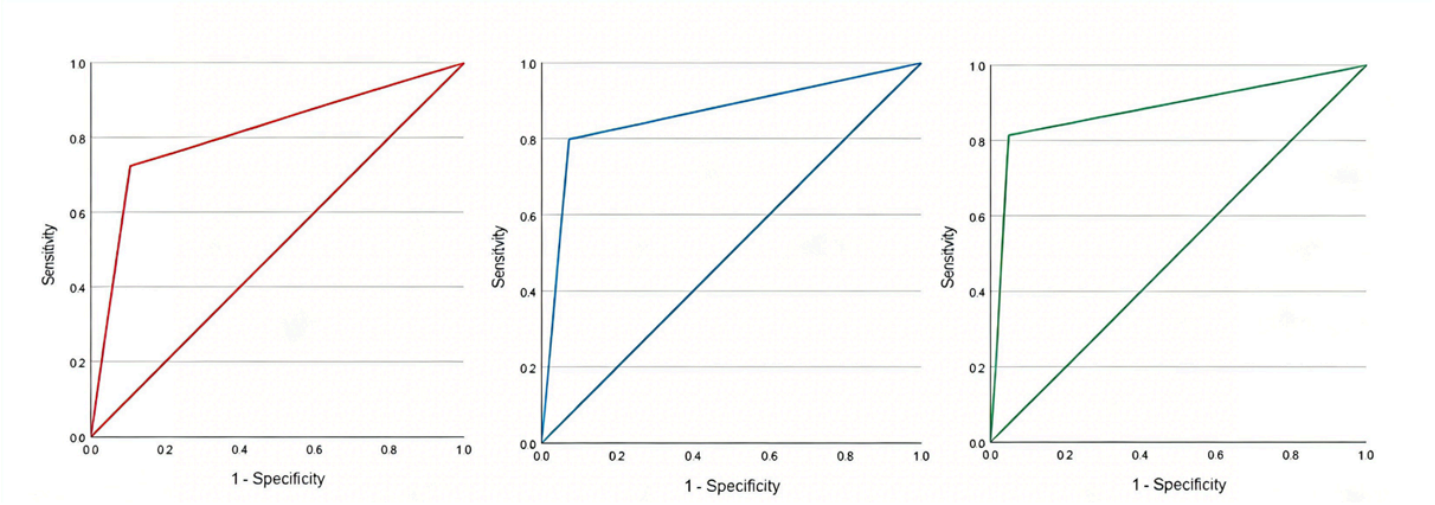


Figure 2

Forest plot of independent risk factors for malignant intraductal breast lesions based on multivariate logistic regression



a：US；b：ABUS；c：US＋ABUS

Figure 3

ROC curves of three diagnostic modalities for differentiating benign and malignant intraductal breast lesions

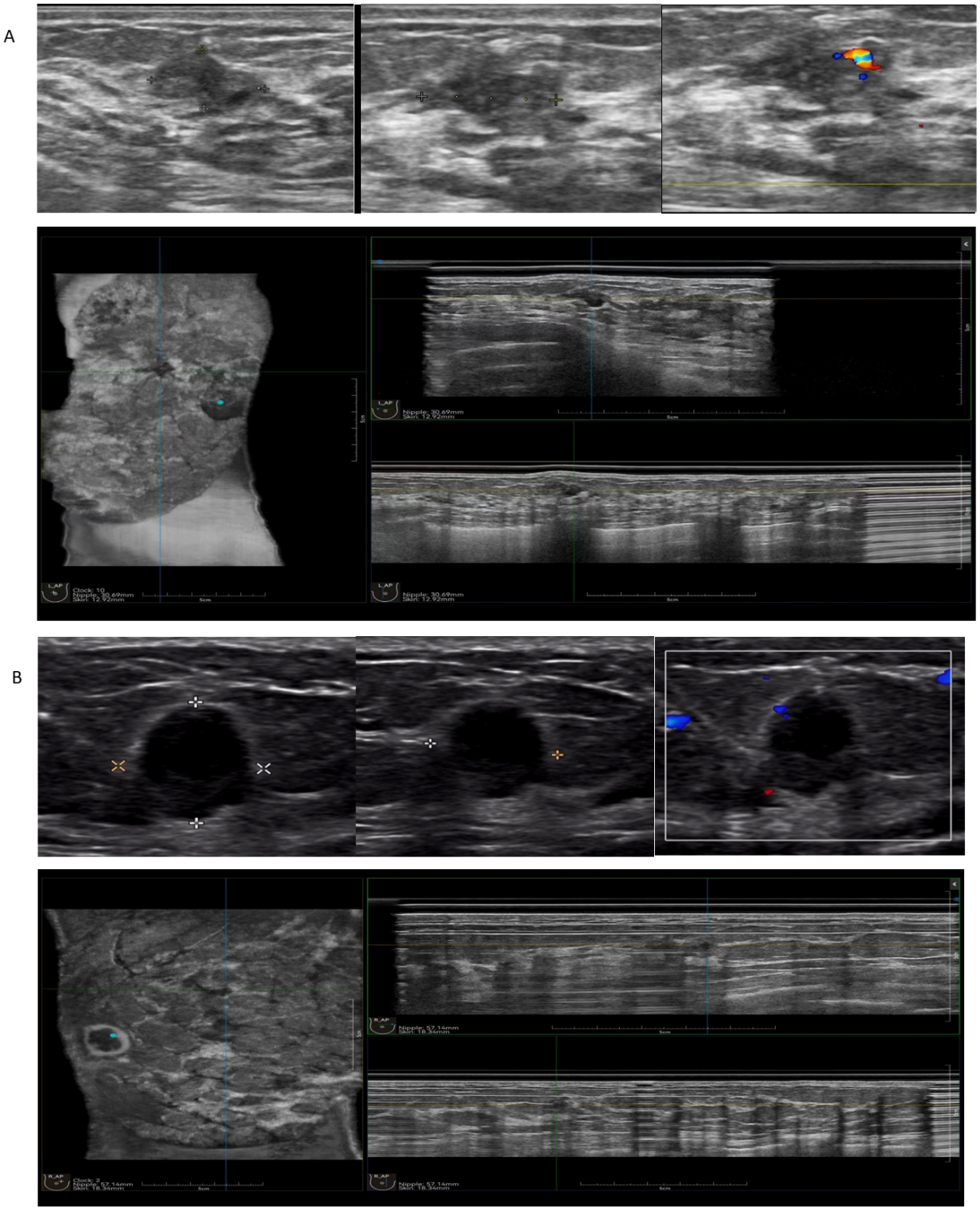


Figure 4

Representative 2D and ABUS images of benign and malignant intraductal breast lesions

Figure A. 2D and ABUS images of ductal carcinoma in situ with microinvasion

Conventional 2D ultrasound revealed a hypoechoic nodule in the left breast with ill-defined margin and irregular shape, seemingly connected to the mammary duct; CDFI detected internal blood flow signals. On ABUS coronal plane, an irregular hypoechoic lesion was seen distributing along the duct, with surrounding breast parenchyma converging toward the lesion center. Postoperative pathology confirmed ductal carcinoma in situ with microinvasion.

Figure B. 2D and ABUS images of intraductal papilloma

2D ultrasound demonstrated a hypoechoic nodule in the left breast with clear boundary, irregular contour and peripheral hyperechoic rim; CDFI showed intralesional blood flow. ABUS displayed a well-demarcated hypoechoic lesion attached to the duct without peripheral parenchymal convergence. Postoperative pathology verified intraductal papilloma.